OPEN ACCESS

Original research

Three-dimensional bioprinted hepatorganoids prolong survival of mice with liver failure

Huayu Yang,[1] Lejia Sun,[1] Yuan Pang,[2,3,4] Dandan Hu,[1,5] Haifeng Xu,[1] Shuangshuang Mao,[2,3,4] Wenbo Peng,[6] Yanan Wang,[7] Yiyao Xu,[1] Yong-Chang Zheng,[1] Shunda Du,[1] Haitao Zhao,[1] Tianyi Chi,[1] Xin Lu,[1] Xinting Sang,[1] Shouxian Zhong,[1] Xin Wang,[8,9,10] Hongbing Zhang,[7] Pengyu Huang,[6,11] Wei Sun,[2,3,4,12] Yilei Mao [1]

► Additional material is published online only. To view please visit the journal online (http://dx.doi.org/10.1136/gutjnl-2019-319960).

For numbered affiliations see end of article.

Correspondence to
Professor Yilei Mao, Department of Liver Surgery, Peking Union Medical College (PUMC) Hospital, PUMC & Chinese Academy of Medical Sciences, Beijing, China; pumch-liver@hotmail.com, Professor Wei Sun, Biomanufacturing Center, Department of Mechanical Engineering, Tsinghua University, Beijing, China; weisun@tsinghua.edu.cn and Professor Pengyu Huang, School of Life Science and Technology, ShanghaiTech University, Shanghai, China; huangpy@shanghaitech.edu.cn

HY, LS, YP and DH contributed equally.

Received 28 September 2019
Revised 28 April 2020
Accepted 6 May 2020
Published Online First 20 May 2020

ABSTRACT

Objective Shortage of organ donors, a critical challenge for treatment of end-stage organ failure, has motivated the development of alternative strategies to generate organs in vitro. Here, we aim to describe the hepatorganoids, which is a liver tissue model generated by three-dimensional (3D) bioprinting of HepaRG cells and investigate its liver functions in vitro and in vivo.

Design 3D bioprinted hepatorganoids (3DP-HOs) were constructed using HepaRG cells and bioink, according to specific 3D printing procedures. Liver functions of 3DP-HOs were detected after 7 days of differentiation in vitro, which were later transplanted into Fah-deficient mice. The in vivo liver functions of 3DP-HOs were evaluated by survival time and liver damage of mice, human liver function markers and human-specific debrisoquine metabolite production.

Results 3DP-HOs broadly acquired liver functions, such as ALBUMIN secretion, drug metabolism and glycogen storage after 7 days of differentiation. After transplantation into abdominal cavity of *Fah*$^{-/-}$*Rag2*$^{-/-}$ mouse model of liver injury, 3DP-HOs further matured and displayed increased synthesis of liver-specific proteins. Particularly, the mice acquired human-specific drug metabolism activities. Functional vascular systems were also formed in transplanted 3DP-HOs, further enhancing the material transport and liver functions of 3DP-HOs. Most importantly, transplantation of 3DP-HOs significantly improved the survival of mice.

Conclusions Our results demonstrated a comprehensive proof of principle, which indicated that 3DP-HO model of liver tissues possessed in vivo hepatic functions and alleviated liver failure after transplantation, suggesting that 3D bioprinting could be used to generate human liver tissues as the alternative transplantation donors for treatment of liver diseases.

Significance of this study

What is already known on this subject?
- Shortage of organ donors is a critical challenge towards treatment of end-stage organ failure.
- Three-dimensional (3D) bioprinting-generated organs in vitro may provide a possible solution.
- However, it still remains a challenge to successfully construct various 3D bioprinting-generated functional organs and to apply them to regenerative medicine.

What are the new findings?
- 3D bioprinted hepatorganoids (3DP-HOs) broadly acquired liver functions, such as ALBUMIN secretion, drug metabolism and glycogen storage after differentiation.
- 3DP-HOs prolonged survival of mice with liver failure and displayed increased synthesis of liver-specific proteins. Particularly, the mice acquired human-specific drug metabolism activities.
- Functional vascular systems were also formed in the 3DP-HOs after transplantation, further enhancing the function of material-transport as well as other functions of 3DP-HOs.

How might it impact on clinical practice in the foreseeable future?
- Our study has clarified the potential value of 3D bioprinting technology in liver transplantation therapy. This technology along with appropriate cells can be used to create artificial organs, which can be transplanted into the body, play normal physiological functions in vivo and provide novel solutions to treat certain diseases.

Check for updates

To cite: Yang H, Sun L, Pang Y, *et al*. *Gut* 2021;**70**:567–574.

INTRODUCTION

Shortage of organ donors, a critical challenge for the treatment of end-stage organ failure, has motivated the development of alternative strategies, such as three-dimensional (3D) bioprinting, to generate organs in vitro.[1 2] Despite many years of development of bioprinting technology, it still remains a challenge to successfully construct various 3D bioprinting-generated functional organs and to apply them to regenerative medicine.[3]

Limited orthotropic liver transplantations, partial extracorporeal hepatic support and narrow-scale treatment by injection of hepatocytes do not meet the medical demands from the ever-expanding end-stage liver disease patients.[4] For decades, numerous efforts have been made to generate functional cells in vitro for potential use in regenerative medicine.[5–9] However, spatial organisation of these cells into functional tissue or organ constructs has remained a major obstacle.[10–13] Important factors

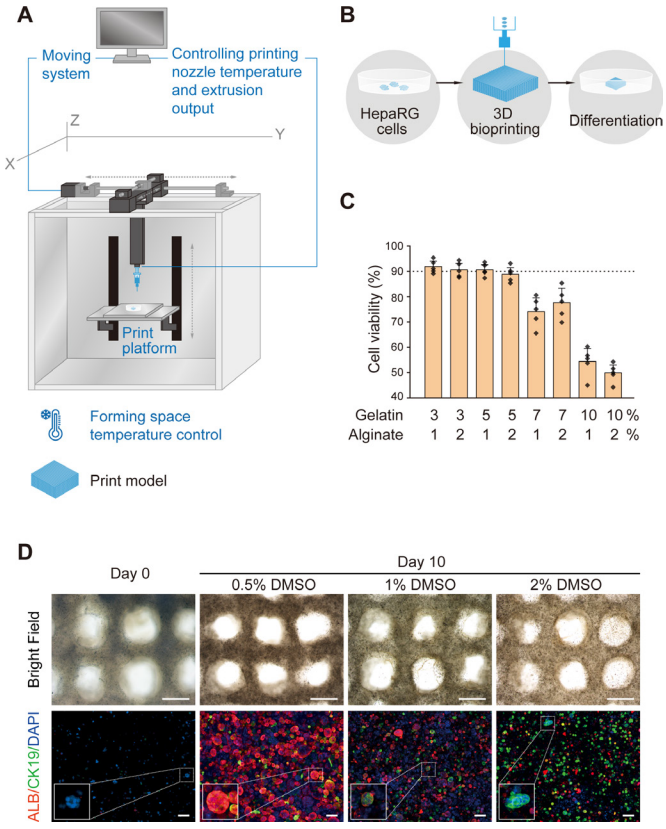

Figure 1 Fabrication of 3D HepaRG/hydrogel mass. (A) Schematic illustration of the 3D cell printer. (B) Schematic illustration of the 3D cell-printing process. (C) Cell viability with various hydrogel compositions of gelatin and alginate. (D) Top view of 3D HepaRG/hydrogel constructs on day 0 (before induction) and day 10 (induced by the indicated concentrations of DMSO). Scale bar: 1 mm. Expressions of hepatocyte marker protein, ALBUMIN (ALB, red) and cholangiocyte marker protein, CK19 (green), were determined by immunofluorescence staining. Scale bar: 100 µm. 3D, three-dimensional; CK19, cytokeratin 19; DMSO, dimethyl sulfoxide.

to construct a reliable hepatic organoid in vitro for implantation include: (1) an adequate cell source with a well-organised structure for further manipulation during implantation, (2) a 3D microenvironment with efficient mass transfer to maintain liver-specific functions that closely match those in vivo and (3) ease of handling and immobilisation during transplantation.

In this study, we describe a liver tissue model generated by 3D bioprinting of HepaRG cells,[14 15] which can be transplanted and is functional in vivo. We designated this model as a 'hepatorganoids'. HepaRG cells, in the form of 3D bioprinted hepatorganoids (3DP-HOs), were differentiated into hepatocytes in vitro; these organoids acquired several liver functions, such as ALBUMIN secretion, drug metabolism and glycogen storage after 7 days of differentiation. After transplantation of 3DP-HOs into abdominal cavities of mice of the *Fah*$^{-/-}$*Rag2*$^{-/-}$ (F/R) liver injury mouse model; the 3DP-HOs further matured and exhibited increased synthesis of liver-specific proteins. In particular, 3DP-HOs acquired characteristics related to human-specific drug metabolism in these mice. Functional vascular systems were also formed in the 3DP-HOs at 14 days after transplantation, further supporting the function of material transport as well as other functions of 3DP-HOs. More importantly, transplantation of 3DP-HOs significantly improved the survival of the treated mice. Thus, our results proved that HepaRG cell-derived 3DP-HOs, modelled on liver tissue, exhibited mature hepatic functions after transplantation and alleviated liver failure in animal recipients. This finding suggests that the 3D bioprinted human liver tissues from normal hepatic cells could be used as alternative transplantation donors for the treatment of liver diseases.

MATERIALS AND METHODS

3D bioprinting and culture of 3DP-HOs

A 3D cell printer (SPP1603) provided by SUNP was employed to fabricate in vitro liver constructs following a previously established method.[16] Briefly, HepaRG cells were harvested and prepared as a suspension in a culture medium. The cell suspension and a 4% sodium alginate solution were mixed at a ratio of 2:1 (v/v). The mixture was incubated at 37°C for 5 min and then mixed with a 20% gelatin solution at appropriate volume ratios, resulting a final cell density of 1×10^6/mL. One mL of the cell/biomaterial mixture was drawn into a sterilised syringe with a 23 G needle and set into the 3D printer at a controlled temperature. The temperatures of both the nozzle and forming chamber were adjusted to determine the optimal conditions for maintaining the highest cell viability during printing. Petri dishes of 35 mm in diameter were precoated with 0.0125‰ (w/v) poly-L-Lysine (P8920; Sigma-Aldrich) to collect the printed structures. Each 3DP-HO was then fabricated by forced extrusion at a 150 mm^3/min extrusion speed in a layer-by-layer fashion. The 3DP-HOs were later immersed in a 100 mM calcium chloride solution for 3 min to cross-link with a sodium alginate solution and then transferred into 3 mL of fully supplemented High Glucose Dulbecco's Modified Eagle Medium. Cell survival in the 3DP-HOs was evaluated immediately after printing to assess the influence of the manufacturing process on cell viability. The initial culture was maintained until day 3, and later the medium was changed to dimethyl sulfoxide (DMSO)-containing medium for differentiation of the immobilised HepaRG cells. Differentiation was induced for 7 days with a change of medium every 2 days, followed by biochemical analyses. The process is presented in figure 1A,B. (Details are shown in online supplementary materials and methods).

In vitro liver function analysis

In vitro liver functions of 3DP-HOs were evaluated by the following methods: levels of ALBUMIN, alpha-1 antitrypsin, factor VII and factor IX secretions were measured by ELISA; protein and mRNA expressions of liver functional markers were detected by immunofluorescence and reverse-transcription-PCR (RT-PCR) and real-time quantitative PCR (qPCR), respectively; CYP1A2 and CYP3A4 activities of 3DP-HOs were evaluated by P450-Glo assays; and liver glycogen storage and uptake functions were determined by periodic acid–Schiff (PAS) staining, DiI-labelled acetylated low-density lipoprotein (DiI-ac-LDL) staining, and indocyanine green (ICG) uptake and release assay. (Details are shown in online supplementary materials and methods).

F/R mice and 3DP-HOs transplantation

All animal procedures were performed according to guidelines laid down by the National Institutes of Health and were approved by the Committee and Institutional Review Board of our hospital.

F/R mice were maintained under specific pathogen-free conditions. They were fed drinking water containing 7.5×10^{-3} mg/mL 2-(2-nitro-4-trifluoro-methylbenzoyl)−1,3-cyclo-hexanedi

one (NTBC, Sigma). The genetic background of the F/R mice was C57Bl6/J*129Sv. After anaesthetising, 3DP-HOs were transplanted into the fossa of the abdominal cavity covered with mesentery. Tacrolimus instead of NTBC was added to the drinking water (7.5×10^{-3} mg/mL) postoperation. Body weight was monitored every week post-transplantation. Surviving recipient mice were sacrificed to collect blood, 3DP-HOs and liver samples at 3–4 weeks after transplantation.

In vivo liver function analysis

Liver function parameters were estimated using an AU 5800 automated analyser (Beckmann) in hospital clinical laboratory. Levels of amino acids and human-specific drug metabolism were assessed for in vivo liver functions. (Details are shown in online supplementary materials and methods).

Statistics

All data were shown as the mean±SD. For most statistical analyses, the unpaired Student's t-test was used in this study. The Mantel-Cox log-rank test was applied for survival analysis. Statistical analysis was performed employing the SPSS 23.0 software (IBM). Differences were considered statistically significant if p values were lower than 0.05. For all the tests, data from at least three independent samples or experiments repeated thrice were used.

RESULTS

Construction of 3DP-HOs

To create a human hepatorganoid that displayed liver functions, we adopted the method of 3D bioprinting because of its advantages to rapidly produce a delicate structure at high resolution and incorporate multiple biomaterials to mimic an in vivo microenvironment (figure 1A). As a consequence of experiences gained through a long-term collection of technological developments related to extracellular matrix, oxygen and nutrient support in 3D culture, various cells are successfully applied through 3D bioprinting to form particular functional tissues or organ assemblies that are also composed of very high cell populations.[17–19]

The liver consists of hepatocytes, cholangiocytes, mesenchymal cells, immune cells, vascular cells and some other rare cell types. Hepatocytes and cholangiocytes contribute to most of the liver functions. Thus, we chose HepaRG cells for their capacity to differentiate into functional hepatocytes and cholangiocytes. Previously, successful 3D bioprinting of HepaRG cells was reported that they could be used to generate a hepatic model with a capacity to be infected with viruses in vitro.[20] On the basis of our previous work, gelatin and alginate were used to generate a bioink because of their biocompatibility, thermosensitivity and cross-linking ability after treatment with calcium chloride[21 22] for maintaining structural stability. To optimise conditions for 3D bioprinting of hepatorganoids, we first tested the bioink with various proportions of gelatin and alginate, as well as printing temperatures. Gelatin at low concentrations in the bioink (3% and 5%) did not demonstrate a significant difference in cell viability during printing. However, cell viability decreased when the bioink contained 7% gelatin. In addition, only half of the cells survived when the proportion of gelatin was increased to 10% in the bioink (figure 1C, online supplementary figure 1 and 2). HepaRG cells contiguously proliferated in the 3D bioprinted constructs during the in vitro culture. We noted that a low proportion of gelatin in the bioink led to higher cell proliferation (online supplementary figure 3). Taking into consideration of the structural formation, cell viability, as well as cell proliferation in prolonged culture, we used 5% gelatin and 1% alginate as a bioink composition.

The increased temperatures of the nozzle and forming space in the 3D cell printer contributed to a slightly higher cell viability, but the differences were not significant. However, an increase in the nozzle temperature may reduce stability of the printed 3D construct because of thermosensitivity of gelatin (online supplementary figures 4 and 5). Therefore, in our subsequent experiments, we printed 3DP-HOs by maintaining temperatures of 20°C in the nozzle and 10°C in the forming space. Each 3DP-HO was in the form of a 12-layered rigid cuboid structure of $10\times10\times3$ mm^3 with interconnected channels of about 500 µm in diameters to facilitate sufficient mass transfer of nutrients and oxygen, and removal of metabolic wastes (online supplementary figure 6).

To simulate physiological conditions, the 3DP-HOs were cultured for 3 days and then induced to differentiate under the stimuli of various compositions of DMSO.[14 23] As shown in the figures, increased concentration of DMSO led to increased cholangiocytic lineage differentiation with increased cytokeratin 19 (CK19) +cells and CK19 mRNA expression (figure 1D, online supplementary figure 7). ALB +cells were most abundant under induction conditions with 0.5% DMSO; the number of cells gradually decreased with an increase in DMSO concentrations. ALB mRNA expression was the highest when induced with 1% DMSO but drastically was reduced after induction with 2% DMSO. Concentrations of liver function-related proteins, such as ALBUMIN, alpha-1 antitrypsin, factor VII and factor IX in culture supernatants of 3DP-HOs under various induction conditions, were evaluate by ELISA assays. We observed that the levels of these proteins were significantly increased in cells induced with 0.5% DMSO compared with those in undifferentiated HepaRG cells (online supplementary figure 8). Notably, HepaRG cells of 3DP-HOs were differentiated into ALB +hepatocytes (82.5%±4.6%) after 7 days of induction with 0.5% DMSO (figure 1D). Additionally, HepaRG cells continuously proliferated after induction with 0.5% DMSO (online supplementary figure 9). However, prolonged differentiation (21 days) of 3DP-HOs reduced cell viability (online supplementary figure 10). Hence, we used 3DP-HOs differentiated in 0.5% of DMSO for 7 days (10 days after bioprinting) for the subsequent in vitro and in vivo analyses.

3DP-HOs liver functions in vitro

To detect liver functions of 3DP-HOs, hepatic specificity of the organoids was further confirmed by assessing the expressions of the liver-specific genes by qPCR analysis. Compared with undifferentiated cells, two-dimensional (2D) culture cells and Matrigel-embedded 3D culture cells, the HepaRG cells in 3DP-HOs that were differentiated in vitro for 7 days expressed the highest levels of hepatic genes (figure 2A). This difference was possibly due to better induction of liver-specific transcription factors, including *FOXA2* and *HNF4A*, in the 3DP-HOs (figure 2B). Liver function-related proteins expressed differently between 3DP-HOs and 2D cultures were detected by immunofluorescence. Protein expressions of ALB, multidrug-resistance-associated protein 2, glutathione s-transferase and CYP3A4 of the HepaRG cells in 3DP-HOs were significantly higher than those of the HepaRG cells in 2D cultures (online supplementary figure 11). Moreover, 3DP-HOs secreted ALBUMIN, alpha-1 antitrypsin, and factor VII at levels comparable to those by primary human hepatocytes (PHHs) (figure 2C). We also observed changes in the concentrations of ALBUMIN, alpha-1

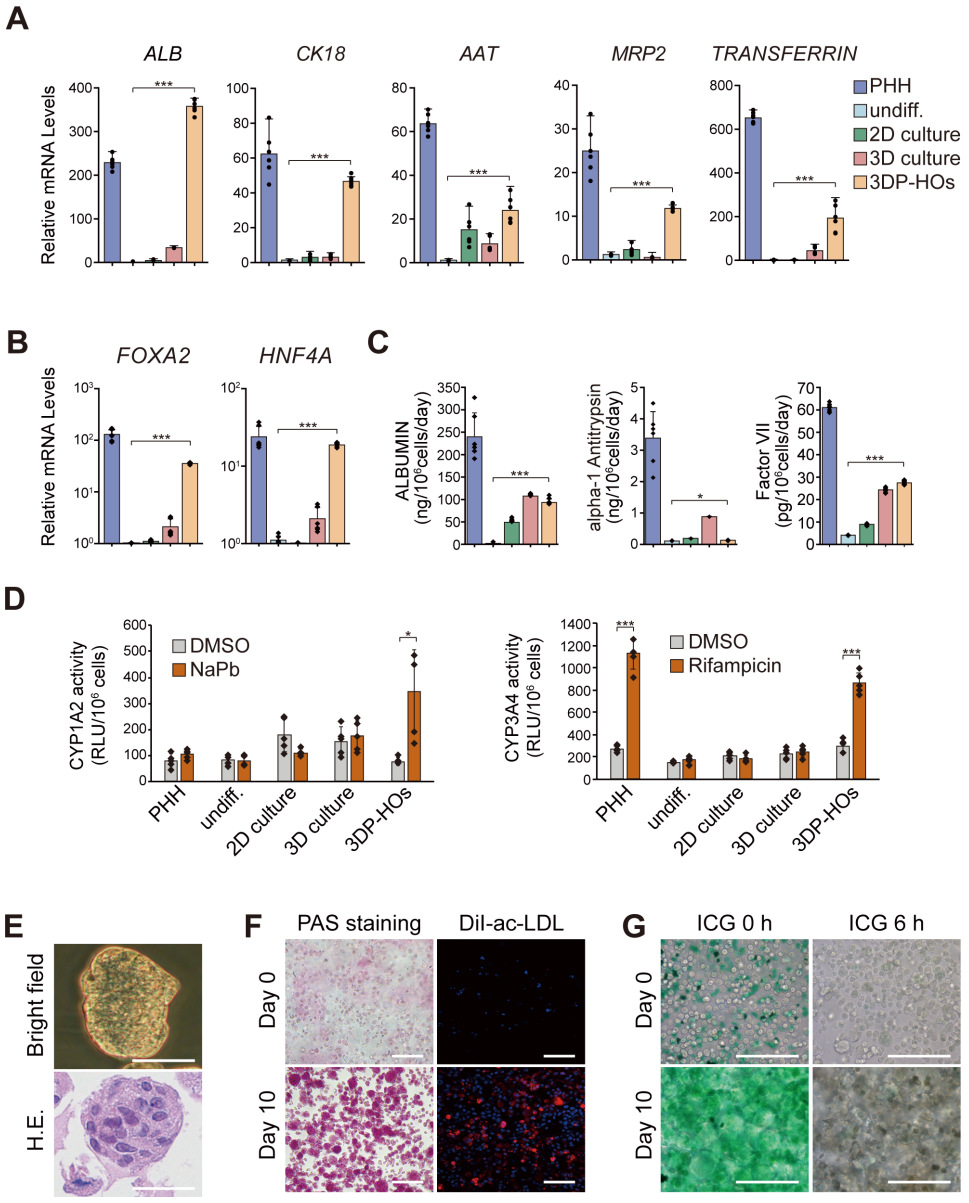

Figure 2 3DP-HOs function in vitro (A, B) Quantitative PCR analysis of hepatic marker gene expression in 3DP-HOs after 7 days of differentiation. Results are represented as mean±SD, n=6. (C) ALBUMIN, alpha-1 antitrypsin, and factor VII levels in culture supernatants were measured by ELISA (n=6). (D) P450-Glo assay of cytochrome activity (CYP1A2, CYP3A4) in 3DP-HOs after 7 days of differentiation. Results are represented as mean±SD (n=5). (E) Microscopic image of a cell mass in a 3DP-HO (bright field). H&E staining of formalin-fixed paraffin-embedded 3DP-HO sections. (F) Glycogen storage determined by PAS staining; DiI-ac-LDL uptake in 3DP-HOs (red). (G) ICG uptake and release in 3DP-HOs (green). Scale bar, 100 µm. *P<0.05; ***P<0.001. 3DP-HOs, three-dimensional bioprinted hepatorganoids; DiI-ac-LDL, DiI-labelled acetylated low-density lipoprotein; DMSO, dimethyl sulfoxide; ICG, indocyanine green; PAS, periodic acid-Schiff; PHH, primary human hepatocytes.

antitrypsin, factor VII and factor IX in culture supernatants of 3DP-HOs, cultured for various time periods in vitro (online supplementary figure 12). Liver functions of 3DP-HOs were the highest after culturing for 2–3 weeks, then gradually declined. However, PHHs, 2D culture cells and Matrigel-embedded 3D culture cells did not survive when cultured for the same time period.

To demonstrate the detoxification function of 3DP-HOs, experiments for extensive in vitro analyses of CYP enzymes were performed. Our results indicated that 3DP-HOs acquired CYP1A2 and CYP3A4 activities at levels that were comparable to those in PHHs (figure 2D). Remarkably, 3DP-HOs responded to some known inducers, such as sodium phenobarbital or rifampicin, to increase the activities of CYP1A2 or CYP3A4. Results revealed that expressions of several CYP450 genes, including *CYP1A2*, *2A6*, *2B6*, *2*C8, *2*C9, *2D6*, *3A4* and *3A11*, were enhanced after treatment with 3-methylcholanthrene, sodium phenobarbital or rifampicin (online supplementary figure 13). Therefore, we proved that 3DP-HOs expressed various CYP450 genes and that such gene expressions could be further induced to higher levels after treating them with inducers.

Morphologically, cells in 3DP-HOs grew in the form of clumps (figure 2E). Cells in a hepatorganoid accumulated glycogen aggregates as shown by PAS staining (figure 2F). ICG uptake and release (figure 2G) and DiI-ac-LDL importation were also found in the 3DP-HOs (figure 2F). These results suggested that 3DP-HOs acquired the sufficient levels of hepatic functions in vitro after DMSO-induced differentiation.

3DP-HOs transplantation rescues Fah-deficient mice

To analyse the functionality of 3DP-HOs in vivo, we transplanted 3DP-HOs into abdominal cavities of F/R mice. The *Fah*$^{-/-}$ mouse model is a well-established model for tyrosinemia type I, a tyrosine metabolism-deficient disease caused by loss of function of fumaroylacetic acid hydrolase. *Fah*$^{-/-}$ mice were administered NTBC in drinking water to suppress the accumulation of toxic metabolites of tyrosine in hepatocytes.[24 25] It is observed that after NTBC withdrawal (NTBC-off), *Fah*$^{-/-}$ mice undergo liver failure and die. To avoid immunological rejection, we used F/R mice, which were established and used in our previous work.[26] Immediately after 3DP-HOs transplantation, NTBC administration was discontinued to induce chronic liver injury in F/R mice.[25] Tacrolimus (7.5×10^{-3} mg/mL) was orally administrated daily to further suppress immunological reactions. F/R mice that received 3DP-HOs had significantly prolonged survival and decreased body weight loss (figure 3A,B). At 4 weeks after transplantation, the serum levels of alanine aminotransferase, total bilirubin, direct bilirubin, gamma-glutamyl transpeptidase and alkaline phosphatase were decreased significantly, suggesting that the 3DP-HOs transplantation alleviated injury of the liver (figure 3C). Histological analysis further confirmed that the mice livers maintained intact liver structures with reduced necrotic-like injuries after 3DP-HOs transplantation (online supplementary figure 14). Furthermore, 3DP-HOs transplantation improved liver functions as observed by increased serum levels of mouse ALBUMIN, total protein and prealbumin (figure 3C). To investigate the mechanisms that prolong the survival of F/R mice, we examined the levels of amino acids in mouse serum. Levels of glutamic acid, citrulline, valine, methionine, isoleucine, leucine, tyrosine and hydroxyproline were reduced considerably in F/R mice that underwent 3DP-HOs transplantation compared with those in sham-operated mice (figure 3D).

The blood vascular system is a critical system that supplies nutrients and oxygen to tissues. Although blood vessels were not included during 3D bioprinting, we noted that the 3DP-HOs transplants started becoming neovascularised at day 14 after transplantation (data are not shown). By infusing fluorescein-conjugated dextran, the neovascular system was clearly visualised in a 3DP-HOs transplant at 4 weeks after transplantation (figure 4A,B, online supplementary figures 15-17). Histological analysis also revealed microvessels in the 3DP-HOs transplants (online supplementary figure 15). Immunofluorescence staining further confirmed the expression of mouse CD31 in the 3DP-HOs transplants, suggesting that the vascular systems were mouse derived (online supplementary figure 16). Thus, the 3DP-HOs transplants were functional as well as neovascularised in vivo, which ensured prolonged functions of the 3DP-HOs (online supplementary figures 17–18).

Next, we sacrificed the 3DP-HOs transplanted F/R mice at 4 weeks after transplantation to analyse the functions of 3DP-HOs transplants. Differentiated HepaRG cells in the 3DP-HOs transplants expressed human ALBUMIN (figure 4B). Importantly, significant amounts of human ALBUMIN, alpha-1 antitrypsin, factor VII and factor IX were also detected in the serum of mice transplanted with 3DP-HOs for 4 weeks (figure 4C). To analyse drug metabolism activity, F/R mice transplanted with 3DP-HOs were challenged with debrisoquine, which is readily metabolised in humans but not in mice. After the drug treatment, production of human-specific metabolite 4-hydroxydebrisoquine (4-OH-DEB) was significantly higher in serum samples collected from the mice transplanted with 3DP-HOs (figure 4D).

DISCUSSION

As an attractive and promising technology, 3D bioprinting has being employed in the development of functional physiological tissues/organs in recent years, including bones, heart, kidneys, blood vessels and so on.[27 28] Based on previous reports,[15 29] we used HepaRG, a commonly used hepatic progenitor cell line, to construct a human liver tissue by 3D bioprinting and first applied it to prolong the survival of mice with liver failure. Our findings indicated that the transplanted 3DP-HOs could effectively undertake in vivo hepatic differentiation from early to maturation stages of liver organogenesis and alleviated liver failure of the animal recipients after transplantation. These findings also suggested that 3D bioprinting-generated liver tissues from normal human hepatic cells may play an important role in the treatment of terminal liver diseases.

In the process of continuously optimising the printing process, we found that the concentration of bioink, temperature of the nozzle and forming space have an important influence on the survival rate of the cells and durability of the 3D structure. After experimenting with several different conditions, the existing printing process parameters were determined. The in vitro liver model was fabricated into a rigid cuboid structure of $10\times10\times3$ mm^3 (12 layers) in size, with interconnected channels of about 500 µm in diameter, taking into account the fact that cells reside less than 200 µm from the nearest blood vessels, in vivo, due to the limitation in oxygen diffusion.[30]

Based on our preliminary study, HepaRG cells were selected from several cell candidates for 3D bioprinting in consideration of cell viability after bioprinting process. Recently, it was reported that HepaRG cells could be used in 3D bioprinting to generate a hepatic model capable of being infected with viruses in vitro.[20] In present study, we showed a significant improvement of the 3D bioprinting of hepatic tissues. In our process, HepaRG cells demonstrated steady growth in the 3D bioprinted constructs, which gradually formed spheroids during the 7 days of culture (online supplementary figure 19). Notably, both ALBUMIN expression and CYP3A4 activities of the 3DP-HOs were comparable to the levels of PHHs. As proved by our results, the 3D bioprinting process and bioink used in the current study were optimised and selected after performing several pre-experiments, to achieve higher growth, viability and functionality of the cells.

In this study, HepaRG cells rapidly proliferated and converted into spheroids and presented a clonogenic growth potential in the 3D-printed model than those grown as a monolayer. Moreover, more advanced spheroids were maintained in the 3D-printed model (figure 1) due to a mass transfer through an interconnected grid structure, where there was a sufficient and continuous oxygen supply to the cells embedded in the printed construct from different directions. However, HepaRG cells in the sandwich culture exhibited a non-uniform 3D cluster formation and distribution, because oxygen could only be supplied from the top side and metabolic waste easily accumulated inside the hydrogel, resulting in a culture condition of insufficient mass transfer (online supplementary figure 19). The growth of cell clusters in 3D culture systems constructed in different ways and the matrix was further examined. It was found that the diameter of the cell clusters in the 3DP-HOs group was significantly larger than that of the bioink as the 3D sandwich culture matrix group and Matrigel as the 3D sandwich culture matrix group after 7 days culture in vitro (online supplementary figure 19). This result indicates that the cell culture milieu constructed by 3D bioprinting is more conducive to proliferation and differentiation of HepaRG cells, which in turn lays a foundation for

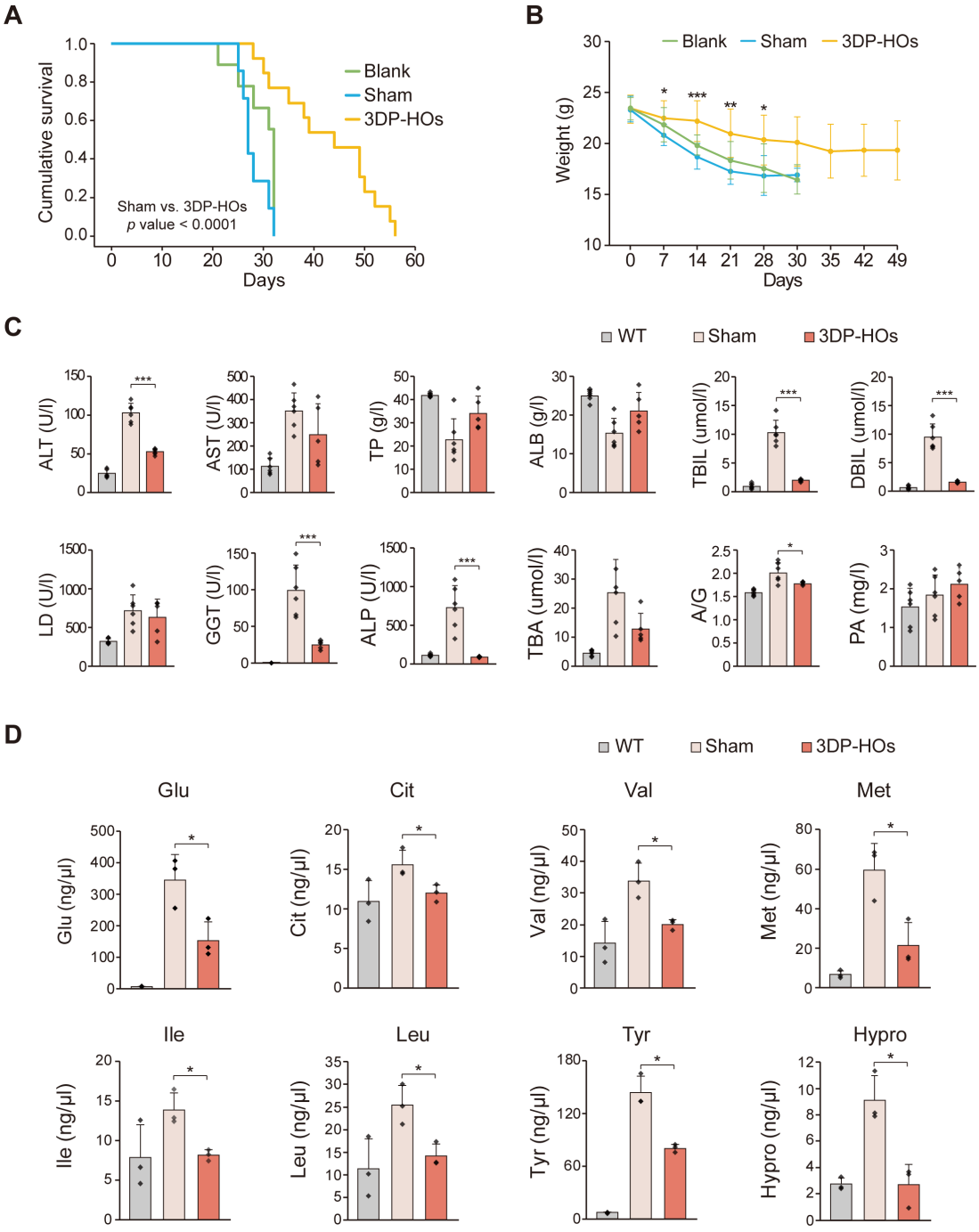

Figure 3 Transplantation with 3DP-HOs rescues *Fah*$^{-/-}$*Rag2*$^{-/-}$ (F/R) deficient mice. (A) Kaplan-Meier survival curve of 3DP-HOs-transplanted mice (n=13), sham-operated F/R mice (n=7), and control F/R mice (n=9) after NTBC withdrawal. (B) Body weight was measured every week after NTBC withdrawal. Data are presented as mean±SD, t-test. (C) Serum levels of alanine aminotransferase (ALT), aspartate aminotransferase (AST), total protein (TP), ALB, direct bilirubin (DBIL), lactic dehydrogenase (LD), gamma-glutamyl transpeptidase (GGT), alkaline phosphatase (ALP), total bile acid (TBA), albumin/globulin ration (A/G) and prealbumin (PA) in wild type (n=6), sham-operated F/R mice (n=6) and 3DP-HOs-transplanted F/R mice (n=5, sera collected at 4 weeks after transplantation). Data are presented as mean±SD, t-test. (D) Serum levels of the indicated amino acids in wildtype (n=3), sham-operated F/R mice (n=3) and 3DP-HOs-transplanted F/R mice (n=3, sera collected at 4 weeks after transplantation), t-test. *P<0.05; **P<0.01; ***P<0.001. ALB, albumin; 3DP-HOs, three-dimensional bioprinted hepatorganoids.

further development of liver cell functions. This finding was further confirmed by in vitro liver functions of 3DP-HOs. When HepaRG cell-derived 3DP-HOs were compared with 2D tissue structures in culture, the expression levels of all the hepatic genes and liver-specific transcription factors in 3DP-HOs were higher than those of 2D structures, and the levels of protein secretion and detoxification functions were also higher.

After the well-maintained growth and functions of 3DP-HOs were proved in in vitro experiments, they were transplanted into mice; the survival time of the mice was significantly prolonged, especially those showing the presence of blood vessels in the 3DP-HOs. Each recipient was transplanted with a 3DP-HO containing approximately 5×10^5 hepatocytes in the abdominal cavity. Active liver functions through these

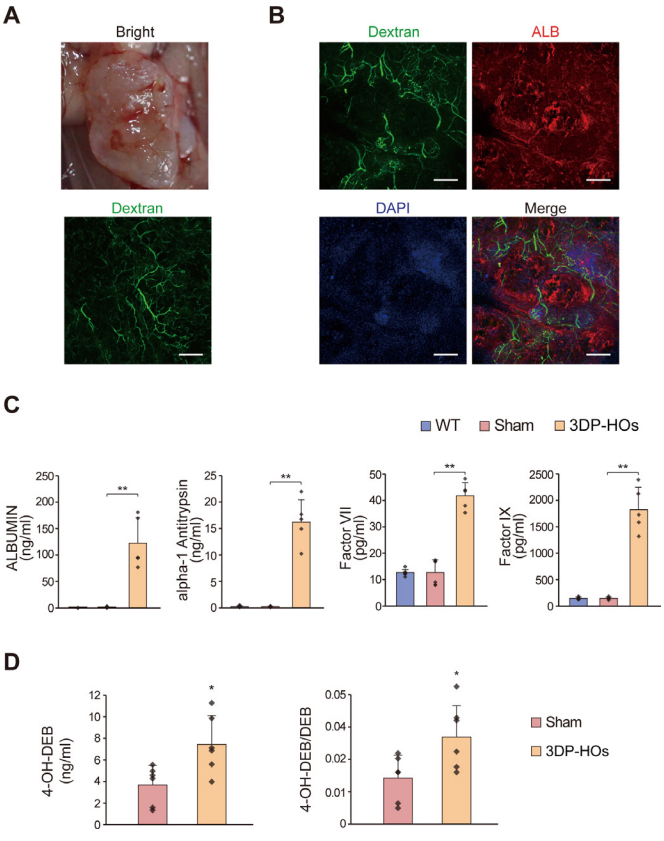

Figure 4 Human liver functions of 3DP-HOs in *Fah*$^{-/-}$*Rag2*$^{-/-}$ (F/R) mice. (A) Macroscopic observation of transplanted 3DP-HOs (upper panel). The vascular system is shown after dextran infusion. Scale bar, 500 µm. (B) Figure depicts dextran infusion displaying functional vessel formation and red fluorescence showing human ALB expression at 4 weeks. scale bar, 200 µm. (C) Serum levels of human ALBUMIN, alpha-1 antitrypsin, factor VII and factor IX were measured by ELISA in wild type (n=6), sham-operated F/R mice (n=6), 3DP-HOs-transplanted F/R mice (n=5, sera collected at 4 weeks after transplantation), t-test. (D) Human-specific debrisoquine metabolite production (mean±SD, n=6, t-test). *P<0.05; **P<0.01. 3DP-HOs, three-dimensional bioprinted hepatorganoids.

transplanted hepatocytes alleviated liver damage in F/R mice and prolonged their survival. It is well known that the hepatocytes are very robust, and a limited number of cells are capable of performing biological functions of the entire body. The liver accounts for 3%–5% of body weight in humans. For adults weighing 60 kg, the liver weight is about 1.5–2 kg, of which the number of hepatocytes is about 3.57×10^{11}, accounting for 1% of the total number of cells in the human body.[31] The liver weight of an adult mouse is about 5.2 g, accounting for 26.0% of the total body weight and approximately has 7×10^{8} hepatocytes.[32] Prolonging the lifespan of liver-deficient mice requires a certain number of hepatocytes for normal catabolism. The 5×10^{5} human hepatocytes contained in the 3DP-HOs were sufficient to play this role, thus proving that these human hepatocytes had suitable liver-related functions. A large number of cell manipulations and accumulation of cells can lead to cell death if there are no blood vessels to transfer sufficiency oxygen and nutrients. However, in 3DP-HOs, cells were embedded in an oxygen-permeable hydrogel with interconnected lattice structure, which promoted a mass transfer to maintain cellular viability and function. Therefore, even with a relatively small number of cells and low cell density, the 3D bioprinted constructs functioned very well.

To generate a transplantable 3D bioprinting-generated liver organ for clinical therapy is still a long-term goal. However, we successfully accomplished an important step -- the first step to prove that 3DP-HOs have in vivo hepatic functions and also that transplanted 3DP-HOs can rescue liver failure in a mouse model. It should be mentioned that our study is limited by the fact that we used only one type of hepatic cells, the HepaRG cell lines, for the construction of 3DP-HOs, to demonstrate our proof of concept. By and large, the state-of-art 3D bioprinting technique is still in early stages of research and development. During the initial stages of our study, we tested several hepatic cells for 3D bioprinting, including PHHs, fetal liver cells, modified hepatoma cell line HepG2-GS-CYP3A4 and HepaRG cells. However, most of them did not have the necessary characteristics to be used in this relatively complicated process. Particularly, the survival rate of PHHs after printing was too low (less than 10%), and the in vitro liver functions of foetal liver cells and HepG2 cell lines were also not satisfactory. Among all these tested primary cells and cell lines, the HepaRG cell line is the most appropriate alternative to PHHs, because it possesses comparable metabolic and morphological properties. Hence, it is frequently utilised in metabolic or cell biology studies.[14 15] In our subsequent studies, therefore, HepaRG cells were mainly selected for bioprinting, although other cells were used partially in this study to further support our proof of concept. We realise that HepaRG cells cannot be used directly in humans, but our data overall confirms the superiority of our methods in establishing 3D bioprinting-generated liver tissues or organs and their clinical potential. It is believed that with development in the fields of medicine and biology in the future, more suitable cells will be available as tissue-specific donor cells or seed cells for bioengineering, such as various induced pluripotent stem cells-derived tissue-specific cells. Specifically, for our research, development of the technology related to in vitro manipulation of cultured human hepatocytes will significantly help us to create improved clinically transplantable 3D bioprinted liver tissues or organs, which in turn will assist in the development of new clinical methods to treat liver diseases.

In summary, we significantly modified the 3D bioprinting process and successfully printed a stable 3D liver organoid in vitro, which performed systematic liver functions both in vitro and in vivo. Employing transplantation assays, we demonstrated a proof of principle towards the application of 3D bioprinted human liver tissues as transplantation donors. Besides their use in clinical transplantation, they may also be applied to serve as a rescue bridge for transition of liver failure to liver regeneration or act as a supplement towards extensive hepatectomy resection and temporary maintenance of the liver during a waiting period for transplantation.

Author affiliations
[1]Department of Liver Surgery, Peking Union Medical College (PUMC) Hospital, PUMC & Chinese Academy of Medical Sciences, Beijing, China
[2]Biomanufacturing Center, Department of Mechanical Engineering, Tsinghua University, Beijing, China
[3]Biomanufacturing and Rapid Forming Technology Key Laboratory of Beijing, Tsinghua University, Beijing, China
[4]Overseas Expertise Introduction Center for Discipline Innovation, Tsinghua University, Beijing, China
[5]Department of Hepatobiliary Surgery, Sun Yat-sen University Cancer Center, Guangzhou, Guangdong, China
[6]School of Life Science and Technology, ShanghaiTech University, Shanghai, China

[7]State Key Laboratory of Medical Molecular Biology, Department of Physiology, Institute of Basic Medical Sciences, Chinese Academy of Medical Sciences and School of Basic Medicine, Peking Union Medical College, Beijing, China
[8]Research Center for Laboratory Animal Science, Inner Mongolia University, Hohhot, Inner Mongolia, China
[9]Hepatoscience Section, Cell Lab Tech Inc, Sunnyvale, California, USA
[10]Department of Laboratory Medicine and Pathology, University of Minnesota, Minneapolis, Minnesota, USA
[11]Center for Excellence in Molecular Cell Science, Chinese Academy of Sciences, Shanghai, China
[12]Department of Mechanical Engineering, Drexel University, Philadelphia, Pennsylvania, USA

Contributors YM, WS and PH conceived the project. HY, LS, YP and DH performed most of the experiments. YP and SM optimised the printing process of 3DP-HOs. YW, YX, YZ and SD analysed the in vitro functions of 3DP-HOs. HZhao and TC analysed gene expression of 3DP-HOs. XL, XS, SZ, XW and HZhang designed the experiments to characterize in vivo functions of 3DP-HOs. HY, LS, HX and WP performed the in vivo experiments. HY, LS, YM, WS and PH analysed the data. HY, PH, HZhang and YP wrote the manuscript.

Funding This work was supported by grants from the National High-tech Research and Development Projects (863) (no.2015AA020303), National Basic Research Program of China 973 Program Grants (2015CB553802) and CAMS Innovation Fund for Medical Sciences (CIFMS) (No.2016-I2M-1-001). This work was also supported by grants from Strategic Priority Program (SPP) on Space Science (no. XDA15014300), 111 Project (no. B17026), the Ministry of Science and Technology of China (MOST; 2019YFA0801501, 2016YFA0100500), the National Natural Science Foundation of China (NSFC; 31970687, 31571509, 31522038, 51805294, 81730078), ShanghaiTech start-up grant to Pengyu Huang and International Science and Technology Projects (2016YFE0107100).

Competing interests The 3D bioprinter was provided by HEALTH Biomed Company.

Patient and public involvement Patients and/or the public were not involved in the design, or conduct, or reporting, or dissemination plans of this research.

Patient consent for publication Not required.

Provenance and peer review Not commissioned; externally peer reviewed.

Data availability statement All data relevant to the study are included in the article or uploaded as online supplementary information. Other data are available on reasonable request.

ORCID iD
Yilei Mao http://orcid.org/0000-0003-0449-4223

REFERENCES

1 Fisher RA. Living donor liver transplantation: eliminating the wait for death in end-stage liver disease? *Nat Rev Gastroenterol Hepatol* 2017;14:373–82.
2 Tanaka K. Resection versus transplantation for hepatocellular carcinoma exceeding Milan criteria within increasing donor shortage. *Hepatobiliary Surg Nutr* 2017;6:280–3.
3 Vijayavenkataraman S, Yan W-C, Lu WF, *et al*. 3D bioprinting of tissues and organs for regenerative medicine. *Adv Drug Deliv Rev* 2018;132:296–332.
4 Bernal W, Jalan R, Quaglia A, *et al*. Acute-On-Chronic liver failure. *Lancet* 2015;386:1576–87.
5 Huang P, Zhang L, Gao Y, *et al*. Direct reprogramming of human fibroblasts to functional and expandable hepatocytes. *Cell Stem Cell* 2014;14:370–84.
6 Si-Tayeb K, Noto FK, Nagaoka M, *et al*. Highly efficient generation of human hepatocyte-like cells from induced pluripotent stem cells. *Hepatology* 2010;51:297–305.
7 Banas A, Teratani T, Yamamoto Y, *et al*. Adipose tissue-derived mesenchymal stem cells as a source of human hepatocytes. *Hepatology* 2007;46:219–28.
8 Zhang K, Zhang L, Liu W, *et al*. *In Vitro* Expansion of Primary Human Hepatocytes with Efficient Liver Repopulation Capacity. *Cell Stem Cell* 2018;23:806–19.
9 Fu G-B, Huang W-J, Zeng M, *et al*. Expansion and differentiation of human hepatocyte-derived liver progenitor-like cells and their use for the study of hepatotropic pathogens. *Cell Res* 2019;29:8–22.
10 Huch M, Dorrell C, Boj SF, *et al*. *In vitro* expansion of single Lgr5+ liver stem cells induced by Wnt-driven regeneration. *Nature* 2013;494:247–50.
11 Takebe T, Sekine K, Enomura M, *et al*. Vascularized and functional human liver from an iPSC-derived organ bud transplant. *Nature* 2013;499:481–4.
12 Ma X, Qu X, Zhu W, *et al*. Deterministically patterned biomimetic human iPSC-derived hepatic model via rapid 3D bioprinting. *Proc Natl Acad Sci U S A* 2016;113:2206–11.
13 Hu H, Gehart H, Artegiani B, *et al*. Long-Term expansion of functional mouse and human hepatocytes as 3D organoids. *Cell* 2018;175:1591–606.
14 Gripon P, Rumin S, Urban S, *et al*. Infection of a human hepatoma cell line by hepatitis B virus. *Proc Natl Acad Sci U S A* 2002;99:15655–60.
15 Anthérieu S, Chesné C, Li R, *et al*. Optimization of the HepaRG cell model for drug metabolism and toxicity studies. *Toxicol In Vitro* 2012;26:1278–85.
16 Ouyang L, Yao R, Zhao Y, *et al*. Effect of bioink properties on printability and cell viability for 3D bioplotting of embryonic stem cells. *Biofabrication* 2016;8:035020.
17 Li Y, Li L, Chen Z-N, *et al*. Engineering-derived approaches for iPSC preparation, expansion, differentiation and applications. *Biofabrication* 2017;9:032001.
18 Swaminathan S, Hamid Q, Sun W, *et al*. Bioprinting of 3D breast epithelial spheroids for human cancer models. *Biofabrication* 2019;11:025003.
19 Meng F, Meyer CM, Joung D, *et al*. 3D Bioprinted *In Vitro* Metastatic Models via Reconstruction of Tumor Microenvironments. *Adv Mater* 2019;31:e1806899:1806899.
20 Hiller T, Berg J, Elomaa L, *et al*. Generation of a 3D liver model comprising human extracellular matrix in an Alginate/Gelatin-Based Bioink by extrusion Bioprinting for infection and transduction studies. *Int J Mol Sci* 2018;19:3129.
21 Zhao Y, Li Y, Mao S, *et al*. The influence of printing parameters on cell survival rate and printability in microextrusion-based 3D cell printing technology. *Biofabrication* 2015;7:045002.
22 Pang Y, Mao SS, Yao R, *et al*. TGF- β induced epithelial–mesenchymal transition in an advanced cervical tumor model by 3D printing. *Biofabrication* 2017;10:044102.
23 Rebelo SP, Costa R, Estrada M, *et al*. Heparg microencapsulated spheroids in DMSO-free culture: novel culturing approaches for enhanced xenobiotic and biosynthetic metabolism. *Arch Toxicol* 2015;89:1347–58.
24 Grompe M, al-Dhalimy M, Finegold M, *et al*. Loss of fumarylacetoacetate hydrolase is responsible for the neonatal hepatic dysfunction phenotype of lethal albino mice. *Genes Dev* 1993;7:2298–307.
25 Overturf K, Al-Dhalimy M, Tanguay R, *et al*. Hepatocytes corrected by gene therapy are selected *in vivo* in a murine model of hereditary tyrosinaemia type I. *Nat Genet* 1996;12:266–73.
26 Huang P, He Z, Ji S, *et al*. Induction of functional hepatocyte-like cells from mouse fibroblasts by defined factors. *Nature* 2011;475:386–9.
27 Mandrycky C, Wang Z, Kim K, *et al*. 3D bioprinting for engineering complex tissues. *Biotechnol Adv* 2016;34:422–34.
28 Grigoryan B, Paulsen SJ, Corbett DC, *et al*. Multivascular networks and functional intravascular topologies within biocompatible hydrogels. *Science* 2019;364:458–64.
29 Leite SB, Roosens T, El Taghdouini A, *et al*. Novel human hepatic organoid model enables testing of drug-induced liver fibrosis *in vitro*. *Biomaterials* 2016;78:1–10.
30 Lovett M, Lee K, Edwards A, *et al*. Vascularization strategies for tissue engineering. *Tissue Eng Part B Rev* 2009;15:353–70.
31 Bianconi E, Piovesan A, Facchin F, *et al*. An estimation of the number of cells in the human body. *Ann Hum Biol* 2013;40:463–71.
32 Sohlenius-Sternbeck A-K. Determination of the hepatocellularity number for human, dog, rabbit, rat and mouse livers from protein concentration measurements. *Toxicol In Vitro* 2006;20:1582–6.